Journal of Physics: Conference Series **2667** (2023) 012022 doi:10.1088/1742-6596/2667/1/012022

The Bethe Ansatz as a Quantum Circuit

Roberto Ruiz[1], Alejandro Sopena[1], Max Hunter Gordon[1,2], Germán Sierra[1] and Esperanza López[1]

[1] Instituto de Física Teórica UAM/CSIC, C/ Nicolás Cabrera 13–15, Universidad Autónoma de Madrid, Cantoblanco, Madrid 28049, Spain
[2] Normal Computing Corporation, New York, New York, USA

E-mail: roberto@ift.csic.es, alejandro.sopena@uam.es, mhuntergordon@gmail.com, german.sierra@csic.es, esperanza.lopez@csic.es

Abstract. The Bethe ansatz is an analytical method to solve exactly solvable models in quantum mechanics. It has been shown that the states of the Bethe ansatz can be prepared by a deterministic quantum circuit whose quantum gates were determined numerically. We report our progress in recasting the Bethe ansatz as a deterministic quantum circuit. We present the analytical expressions of the quantum gates. Formulae rely upon diagrammatic rules that define the wave functions of the Bethe ansatz by matrix product states. Based on the analytical expressions, we prove the unitarity of the quantum gates. We use our results to clarify on the equivalence between the coordinate and algebraic Bethe ansatze in light of matrix-product states.

1. Introduction

The Bethe ansatz is an analytical method to solve exactly solvable models of quantum mechanics. Its initial formulation was the coordinate Bethe ansatz (CBA), which consists of trial functions composed of linear superpositions of plane waves [1]. The algebraic Bethe ansatz (ABA) later systematised the method on the basis of quantum integrability, offering a new perspective on the computation of norms, inner products, and correlation functions. (See [2, 3] for reviews). Further insight on the ABA was gained with the uncovering of its connection with matrix-product states (MPS) [4, 5, 6, 7, 8].

Quantum computing calls for new testing grounds to push the boundaries of quantum supremacy further [9]. Local one-dimensional spin-1/2 quantum chains are suited to the test, for they are under good control. Spin sites of this class of models realise qubits under the identification

$$|\uparrow\rangle := |0\rangle \ , \quad |\downarrow\rangle := |1\rangle \ . \tag{1}$$

However, if the chain is, for instance, gapped, the ground and first excited states obey the area law and have low entanglement entropy [10], hence they can be classically simulated by MPS [11].

To challenge classical computing, highly entangled states must be considered. Quantum integrability is useful in this situation as the Bethe ansatz provides the means to construct eigenstates sistematically (the so-called *Bethe states*). Quantum algorithms for the preparation of Bethe states, with a focus on the XXZ model, have indeed been developed. References [12, 13] presented a probabilistic quantum algorithm which builds upon the CBA to prepare Bethe states. The number of qubits and quantum gates scale polynomially with N, the depth, and M, the number of qubits at $|1\rangle$. However, the success probability decreases exponentially with N for the antiferromagetic ground state with M at $N = \infty$ for arbitrary eigenstates [14].

Reference [15] alternatively developed a deterministic quantum algorithm, called *algebraic Bethe circuit* (ABC), that prepares Bethe states based on the ABA. The number of qubits and quantum gates scale polynomially with N. Reference [15] showed that quantum gates decompose into a layer of matchgates at the non-interacting point, where the XXZ model reduces to the XX model. Nonetheless, no conclusive answer was obtained for the XXZ in general. Since the ABC is the starting point of [16], let us take a closer look on this quantum algorithm.

1.1. The XXZ model

Before we present the ABC, some remarks on the XXZ model are convenient. We impose periodic boundary conditions. The parameters of the XXZ model are the number of spin-chain sites (qubits) N and the anisotropy parameter Δ. The Hamiltonian reads

$$H = J\sum_{j=1}^{N}\left[\sigma_j^1\sigma_{j+1}^1 + \sigma_j^2\sigma_{j+1}^2 + \Delta\left(\sigma_j^3\sigma_{j+1}^3 - 1\right)\right] \ , \tag{2}$$

where J denotes the coupling constant, σ_j^α the α-th Pauli matrix and the j-th site, and $\sigma_{N+1}^\alpha := \sigma_1^\alpha$. Invariance under global $\mathfrak{u}(1)$-symmetry enables M, the number of spin states at $|\downarrow\rangle$ (qubits at $|1\rangle$), to label eigenspaces. Trial wave function of the CBA (*Bethe wave function*) inside the M-th eigenspace carries momenta $p_1, \ldots, p_M$. The Bethe wave function over N qubits with M qubits at $|1\rangle$ is

$$|\Psi_N^{(M)}\rangle = \sum_{1\leq<n_1<\ldots<n_N\leq N}\ \sum_{\substack{a_m=1\\ m=1,\ldots,M}}^{M} \epsilon_{a_1\ldots a_M}\left(\prod_{\substack{p,q=1\\ p>q}}^{M} s_{a_p a_q}\right) x_{a_1}^{n_1-1}\ldots x_{a_M}^{n_M-1}\,|n_1\ldots n_M\rangle \ , \tag{3}$$

where $\epsilon_{a_1\ldots a_M}$ denotes the Levi-Civita symbol with $\epsilon_{1\ldots M}=1$, $x_a := \exp(\mathrm{i}p_a)$, $s_{ab} := 1 + x_a x_b - 2\Delta x_b$, and $|n_1\ldots n_M\rangle = \sigma_{n_1}^-\ldots\sigma_{n_M}^-\,|0_N\rangle$ with $\sigma_j^- = (\sigma_j^1 - \mathrm{i}\sigma_j^2)/2$, and $|0_N\rangle = |0\rangle^{\otimes N}$. The normalised Bethe wave function is

$$|\Phi_N^{(M)}\rangle = \frac{1}{\sqrt{\langle\Psi_N^{(M)}|\Psi_N^{(M)}\rangle}}|\Psi_N^{(M)}\rangle \ . \tag{4}$$

The two-body S-matrix of the model is $S = -s_{12}/s_{21}$. If p_a solve the Bethe equations, Bethe wave functions are Bethe states.

1.2. The Algebraic Bethe Circuit

As we have already mentioned, the ABC is a deterministic quantum algorithm based on the ABA. The ABA uses N physical qubits and M ancillae to produce a state proportional to (3). The building block of the ABA is the R-matrix. We depict the network of the ABA in Figure 1. If one defines $\mathscr{R}_T$ by grouping R-matrices along columns one arrives to Figure 2. QR-factorisation on $\mathscr{R}_T$ eliminates the M ancillae and leads to the ABC. We depict the quantum circuit of the ABC in Figure 3. The ABC produces (3), but normalised. Quantum gates are either long or short.

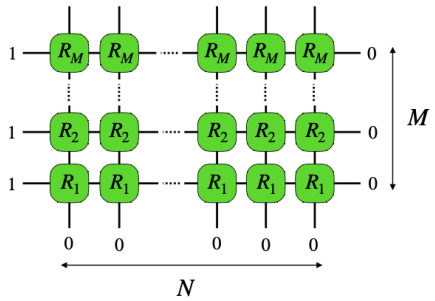

Figure 1. The network of the ABA. There are N physical qubits and M ancillae. The R-matrix R_a depends on p_a. Rounded corners indicate R_a is non-unitary.

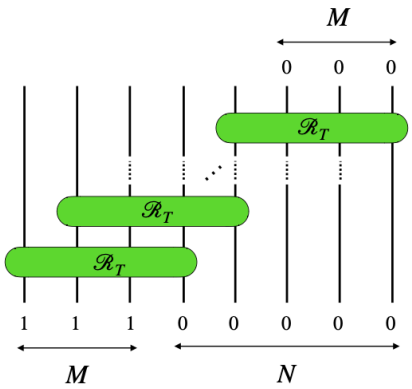

Figure 2. The circuit-like form of the network of the ABA. Grouping R_a along columns yields $\mathscr{R}_T$.

The quantum gates of Figure 3 ultimately follow from a recurrence relation. The recurrence is involved, and [15] provided analytical expressions for $M = 1, 2$, whereas it computed the quantum

gates numerically for $M > 2$. This problem served as a starting point for [16], which obtained closed formulae for the quantum gates of the ABC. The core strategy of [16] was the shift from the MPS of the ABA to the MPS of the CBA. The shift enabled the proposal of an educated guess from which the correct analytical expressions for the quantum gates could be shown to follow. Closed formulae also permitted to prove unitarity. Furthermore, the equivalence between the CBA and the ABA was elaborated on in light of MPS. We convey the chain of equivalences following from the work [15, 16] in Figure 4. The remainder of the text is a report on the results of [16].

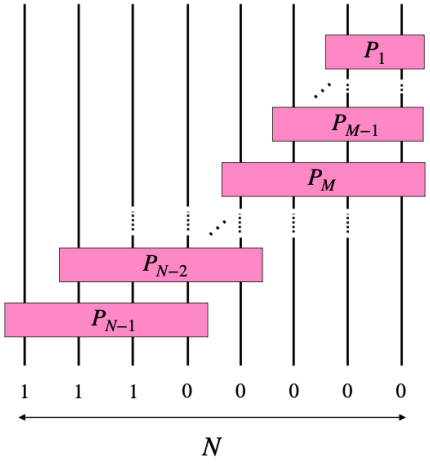

Figure 3. The circuit of the ABC. There are N physical qubits. Quantum gates are short ($1 \leq k < M$) or long ($M \leq k < N$).

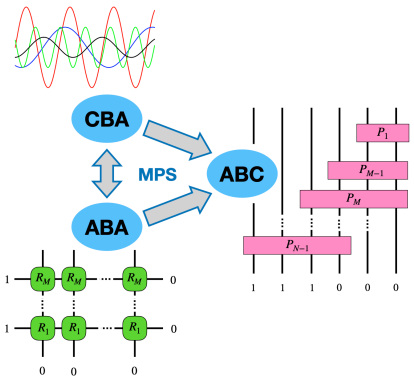

Figure 4. Diagram of results set in [15, 16].

2. Hilbert Space, Symmetry Sectors, and Quantum Gates

The Hilbert space of k qubits is

$$\mathcal{H}_k = \text{lin}\{\, |i_1 ... i_k\rangle : i_a = 0, 1 \,\} = (\mathbb{C}^2)^{\otimes k} \,. \tag{5}$$

The $\mathfrak{u}(1)$-symmetry breaks $\mathcal{H}_k$ into the orthogonal sum of sectors with fixed number of qubits at $|1\rangle$:

$$\mathcal{H}_k = \bigoplus_{r=0}^{k} \mathcal{H}_{r,k} \,, \quad \mathcal{H}_{r,k} = \text{lin}\left\{ |i_1 \dots i_k\rangle : \sum_{a=1}^{k} i_a = r \right\} \,, \quad \dim \mathcal{H}_{r,k} = \binom{k}{r} := d_{r,k} \,. \tag{6}$$

Quantum gates fall into the classes of short and long gates (see Figure 3). Long gates are reducible to isometries, $P_k|0\rangle : \mathcal{H}_M \longrightarrow \mathcal{H}_{M+1}$. Short gates are unitaries, $P_k : \mathcal{H}_{k+1} \longrightarrow \mathcal{H}_{k+1}$. Long and short gates decompose in blocks according to (6). Each block further splits into two blocks according to the state of the leftmost output qubit. Explicitly,

$$P_k|0\rangle = \begin{bmatrix} 1 & 0 & \cdots & 0 \\ 0 & P_k^{(1)} & \cdots & 0 \\ \vdots & \vdots & & \vdots \\ 0 & 0 & \cdots & P_k^{(M)} \\ 0 & 0 & \cdots & 0 \end{bmatrix} \,, \quad P_k = \begin{bmatrix} 1 & 0 & \cdots & 0 & 0 \\ 0 & P_k^{(1)} & \cdots & 0 & 0 \\ \vdots & \vdots & & \vdots & \vdots \\ 0 & 0 & \cdots & P_k^{(k)} & 0 \\ 0 & 0 & \cdots & 0 & 1 \end{bmatrix} \,, \quad P_k^{(r)} = \begin{bmatrix} P_k^{(1,r)} \\ P_k^{(0,r)} \end{bmatrix} \,. \tag{7}$$

where the sector $r = 0$ for long and short gates and $r = M$ for long gates have been normalised to one. We summarise the properties of $P_k^{(i,r)}$ in Table 1.

Table 1. Domain, image, and matrix dimension of the blocks of quantum gates.

$P_k^{(i,r)}$	domain	image	dimension
short	$\mathcal{H}_{r,k+1}$	$\mathcal{H}_{r-i,k}$	$d_{r-i,k} \times d_{r,k+1}$
long	$\mathcal{H}_{r,M}$	$\mathcal{H}_{r-i,M}$	$d_{r-i,M} \times d_{r,M}$

3. The Ansatz for Quantum Gates

The section is devoted to the presentation of the ansatz for the quantum gates. We begin a summary of the basics of MPS. We then consider quantum gates for $M = 1$. The analytical expressions are deducible in this case. We use the previous two subsections to support our ansatz for quantum gates. We conclude the section by proving unitarity. We shall focus on long gates for the sake of clarity and brevity. Short gates are analogous, but display pecularities that, despite their importance, would require an analysis beyond the limits of this report. For a treatment of short gates, we refer to [16].

3.1. The Ansatz for Quantum Gates: Matrix-Product States

Let $\Lambda^i : \mathcal{H}_{\text{anc}} \to \mathcal{H}_{\text{anc}}$ $(i = 0, 1)$ be two matrices over ancillae. The translationally invariant MPS [1] over N qubits that builds upon them reads

$$|\Psi_N\rangle = \sum_{\substack{i_m=0,1 \\ m=1,\dots,N}} \langle\varphi_{\text{in}}| \Lambda^{i_1} \dots \Lambda^{i_N} |\varphi_{\text{out}}\rangle |i_1 \dots i_N\rangle \ , \tag{8}$$

where $|\varphi_{\text{in}}\rangle$ and $|\varphi_{\text{out}}\rangle$ specify the boundary conditions. We depict the network in Figure 5 (with a slight abuse of notation). It is clear from that the network of (8) has linkwise gauge freedom

$$\Lambda^i \mapsto U_k = X_k \Lambda^i X_{k+1}^{-1} \ , \tag{9}$$

which we depict in Figure 6. If the gauge transformation (which in general spoils translation invariance) renders U_k unitary, MPS are said to be in canonical form.

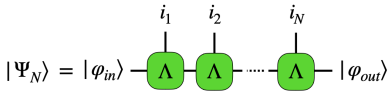

Figure 5. Translationally invariant MPS over N qubits.

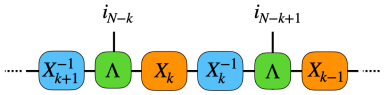

Figure 6. Gauge freedom of the translationally invariant MPS.

3.2. The Ansatz for Quantum Gates: $M = 1$

The quantum circuit ABC with $M = 1$ has just long gates, and $r = 1$ labels its only non-trivial sector. Quantum gates follow from the normalisation constraint of (4) and the unitarity of P_k. Note (3) extends to the definition of the ('partial') Bethe wave function over $1 \leq k < N$ qubits, namely

$$|\Psi_k^{(1)}\rangle = \sum_{n=1}^{k} x^{n-1} |n\rangle \ . \tag{10}$$

We can equivalently deduce $P_k^{(i,1)}$ from the normalisation of $|\Psi_k^{(1)}\rangle$ into $|\Phi_k^{(1)}\rangle$ at each k. The result is

$$\begin{bmatrix} P_k^{(1,1)} \\ P_k^{(0,1)} \end{bmatrix} = \frac{1}{\sqrt{C_{k+1}}} \begin{bmatrix} 1 \\ x\sqrt{C_k} \end{bmatrix} \ , \quad C_k := \langle\Psi_k^{(1)}|\Psi_k^{(1)}\rangle \ , \quad C_k = 1 + |x|^2 C_{k-1} \ , \tag{11}$$

where the last equation above is the recurrence relation we used to write the quantum gates.

[1] The nomenclature is widespread but misleading. Translation invariace actually holds under periodic boundary conditions, not the open boundary conditions we consider in (8).

Table 2. Domain, image, and matrix dimension of the matrices of long gates.

matrix	domain	image	dimension
$B^{(r)}_{k+1}$	$\mathcal{H}_{r,M}$	$\mathcal{H}_{r,M}$	$d_{r,M} \times d_{r,M}$
$\Lambda^{(i,r)}$	$\mathcal{H}_{r,M}$	$\mathcal{H}_{r-i,M}$	$d_{r-i,M} \times d_{r,M}$
$A^{(r-i)}_{k}$	$\mathcal{H}_{r-i,M}$	$\mathcal{H}_{r-i,M}$	$d_{r-i,M} \times d_{r-i,M}$

3.3. The Ansatz for Quantum Gates: $M > 1$
If $M > 1$, the ansatz generalises the results for $M = 1$ via MPS of the CBA.

$$P^{(r,i)}_k = A^{(r-i)}_k \Lambda^{(i,r)} B^{(r)}_{k+1} \ . \tag{12}$$

The ansatz is based on the canonical form of MPS. Consider the matrix over physical qubits and ancillae $\bar{\Lambda} : \mathcal{H}_{\text{anc}} \otimes \mathcal{H}_{\text{phys}} \to \mathcal{H}_{\text{phys}} \otimes \mathcal{H}_{\text{anc}}$. We identify the building block of the MPS as $\bar{\Lambda}^{ib}_{a0} = \Lambda^{i}_{ab}$. Pairs of inverse matrices A_k and B_k put the MPS (8) into canonical form by (6). Finally, the definition

$$\Lambda^0 := \begin{bmatrix} 1 & 0 & \cdots & 0 \\ 0 & \Lambda^{(0,1)} & \cdots & 0 \\ \vdots & \vdots & & \vdots \\ 0 & 0 & \cdots & \Lambda^{(0,M)} \end{bmatrix} , \quad \Lambda^1 := \begin{bmatrix} 0 & \Lambda^{(1,1)} & \cdots & 0 \\ \vdots & \vdots & & \vdots \\ 0 & 0 & \cdots & \Lambda^{(1,M)} \\ 0 & 0 & \cdots & 0 \end{bmatrix} . \tag{13}$$

and the decomposition of A_k and B_k into orthogonal symmetry sectors leads to the ansatz (12).

3.4. The Ansatz for Quantum Gates: Long Gates
We depict the ansatz (12) for long gates in Figure 7. We summarise the properties of the matrices of the ansatz in Table 2. Let us break down each matrix of the ansatz.

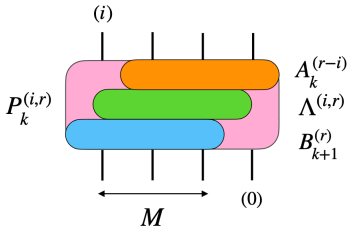

Figure 7. Depiction of the ansatz of long gates.

We begin with $\Lambda^{(i,r)}$. Let the following collective variables in the r-th and the $r-1$-th sector of the k-th gate be

$$x^{(r)}_a = x_{n_1} \dots x_{n_r} \ , \quad x^{(r-1)}_{a'_m} = x_{n_1} \dots x_{n_{m-1}} x_{n_{m+1}} \dots x_{n_r} \ , \quad m = 1, \dots, M \ , \tag{14}$$

respectively. (We refer to [16] for the mapping between $a = 1, \dots, d_{r,k}$ and $1 < n_1 \leq \dots \leq n_r < M$ inside each sector $\mathcal{H}_{r,k}$). The ansatze for $i = 0$ and $i = 1$ read

$$\Lambda^{(0,r)}_{ab} = x^{(r)}_a \delta_{ab} \ , \quad \Lambda^{(1,r)}_{a'_m a} = (-1)^{m-1} s_{n_1 n_m} \dots s_{n_{m-1} n_m} s_{n_{m+1} n_m} \dots s_{n_r n_m} \, x^{(r-1)}_{a'_m} \ . \tag{15}$$

The components follow from digrammatic rules. We illustrate them in Figure 8 and Figure 9.

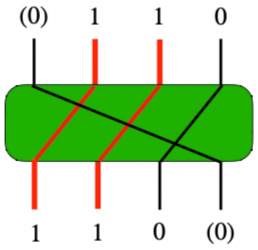

Figure 8. Diagrammatic rules for $\Lambda^{(0,2)}_{11} = x_1 x_2$ for $M = 3$.

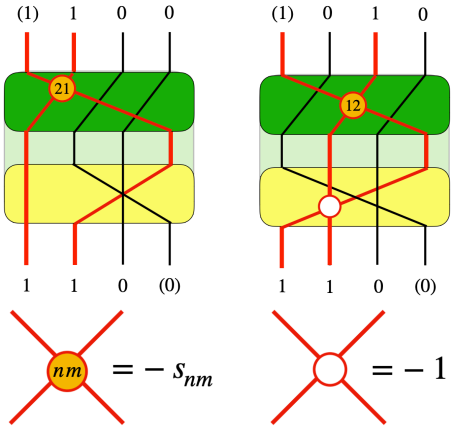

Figure 9. Diagrammatic rules for $\Lambda^{(1,2)}_{11} = -x_1 s_{12} + x_2 s_{21}$ for $M = 3$.

Let us consider $A^{(r)}_k$ and $B^{(r)}_k$. They are inverse matrices. We can clarify the role of these matrices in the light of Subsection 3.2. Just as for the case of $M = 1$, formula (3) extends to the definition of 'partial' Bethe wave functions for every $1 \leq k < N$ if $M > 1$. However, there are multiple Bethe wave functions in the r-th sector at each k as the states carry any $1 \leq r \leq M$ momenta. The highlighted quantum subcircuit of Figure 10 and the highlighted subnetwork of Figure 11 realise $|n_1 \dots n_r\rangle \mapsto |\Phi^{(r)}_{k,a}\rangle$ and $|n_1 \dots n_r\rangle \mapsto |\Psi^{(r)}_{k,a}\rangle$, respectively. Therefore, the normalisation of $|\Psi^{(1)}_k\rangle$ into $|\Phi^{(1)}_k\rangle$ for $M = 1$ tunrs into the orthonormalisation of the non-orthogonal set $|\Psi^{(r)}_{k,a}\rangle$ into $|\Phi^{(r)}_{k,a}\rangle$ for $M > 1$. We stress $|\Phi^{(r)}_{k,a}\rangle$ are not identifiable with normalised Bethe wave functions in general.

The components $A^{(r)}_k$ and $B^{(r)}_k$ admit closed formulae. According to Figure 10 and Figure 11, up to an unitary rotation,

$$|\Phi^{(r)}_{k,b}\rangle = \sum_{a=1}^{d_{r,M}} B^{(r)}_{k,ab} |\Psi^{(r)}_{k,a}\rangle \ , \quad \text{if and only if} \quad B^{(r)\dagger}_k C^{(r)}_k B^{(r)}_k = 1_{d_{r,M}} \quad \text{with} \quad C^{(r)}_{k,ab} := \langle \Psi^{(r)}_{k,b} | \Psi^{(r)}_{k,b} \rangle \ . \tag{16}$$

The matrix equation is the rephrasing of the change of basis into the transformation of the Gram matrix of Bethe wave functions by conjugation. This fact forces the inverse change-of-basis matrix to provide the Cholesky factorisation

$$C^{(r)}_k = A^{(r)\dagger}_k A^{(r)}_k \ . \tag{17}$$

Upper-triangularity and positivity of the diagonal unambigously determine $A^{(r)}_k$, hence its inverse $B^{(r)}_k$. We can thus deduce the following closed formulae, which complete the specification of the ansatz (12):

$$\begin{aligned} A^{(r)}_{k,ab} &= \frac{\det_a C^{(r)}_{k,a\to b}}{\sqrt{\det_{a-1} C^{(r)}_k \det_a C^{(r)}_k}} \ , \quad B^{(r)}_{k,aa} = \sqrt{\frac{\det_{a-1} C^{(r)}_k}{\det_a C^{(r)}_k}} \quad \text{if} \quad a = b \ , \\ B^{(r)}_{k,ab} &= -\frac{\det_{b-1} C^{(r)}_{k,a\to b}}{\sqrt{\det_{b-1} C^{(r)}_k \det_b C^{(r)}_k}} \quad \text{if} \quad a < b \ , \quad B^{(r)}_{k,ab} = 0 \quad \text{if} \quad a > b \ . \end{aligned} \tag{18}$$

3.5. Unitarity

Long gates are unitary if $P_k|0\rangle$ are isometries, as already mentioned. Matrices $P_k|0\rangle$ are unitary in (7) if each block is unitary as well, that is

$$P^{(0,r)\dagger}_k P^{(0,r)}_k + P^{(1,r)\dagger}_k P^{(1,r)}_k = B^{(r)\dagger}_{k+1} \left(\sum_{i=0,1} \Lambda^{(i,r)\dagger} C^{(r-i)}_k \Lambda^{(i,r)} \right) B^{(r)}_{k+1} = 1_{d_{r,M}} \ , \tag{19}$$

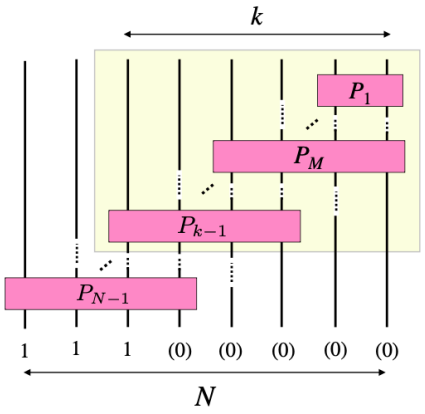

Figure 10. Quantum subcircuit that realises $|n_1 \dots n_r\rangle \mapsto |\Phi^{(r)}_{k,a}\rangle$.

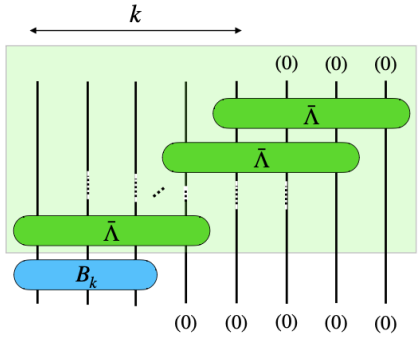

Figure 11. Subnetwork that realises $|n_1 \dots n_r\rangle \mapsto |\Psi^{(r)}_{k,a}\rangle$.

where we used the ansatz (12) and the Cholesky decomposition (17). It follows that the following recurrence relation must hold:

$$C^{(r)}_{k+1} = \sum_{i=0,1} \Lambda^{(i,r)\dagger} C^{(r-i)}_{k} \Lambda^{(i,r)} \ . \tag{20}$$

The recurrence relation holds identically, thus proving unitarity of long gates.

4. ABA = CBA

In this section, we use MPS to expound on the equivalence between the ABA and the CBA. The matrix $\mathscr{R}_T$ in Figure 1 permits us to consider Bethe wave functions of the translationally invariant MPS based on the matrices Γ^i $(i = 0, 1)$, which we represent in Figure 12.

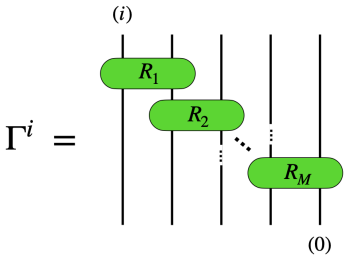

Figure 12. The matrix that defines translationally invariant MPS for the ABA.

Each R-matrix R_a in Figure 12 solely depends on p_a, and reads

$$R_a = \begin{bmatrix} 1 & 0 & 0 & 0 \\ 0 & s_{aa} & x_a & 0 \\ 0 & x_a & s_{aa} & 0 \\ 0 & 0 & 0 & 1 \end{bmatrix} \ , \quad s_{aa} = 1 + x_a^2 - 2\Delta\, x_a \ . \tag{21}$$

We emphasise R_a satisfies the Yang-Baxter equation if and only if s_{aa} and x_a are related as written in (21).

Much alike the quantum gates of the ansatz (12), quantum gates of the ABC of [15] follow from the transformation of the MPS of the ABA into canonical form:

$$P^{(i,r)}_{k} = \mathscr{A}^{(r-i)}_{k}\, \Gamma^{(i,r)}\, \mathscr{B}^{(r)}_{k+1} \ .$$

The pair $\mathscr{A}_k$ and $\mathscr{B}_k$ consists of inverse matrices. The matrix $\mathscr{A}_k$ provides the Cholesky factorisation of $\mathscr{C}_k$, in parallel to (17). The matrices $\mathscr{C}_k$ satisfy recurrence relation like (20). Nonetheless, being involved, the recurrence relation compelled [15] to resort to numerical calculation to solve them. This situation contrasts with that posed by the recurrence relation (20), which can be explicitly worked out.

Canonical MPS of the ABA and the CBA in [15] and in [16] are related. Since both classes of MPS realise the same state, it follows there exist a matrix X such that

$$\Gamma^i = X^{-1}\Lambda^i X \ , \quad \mathscr{A}_k = A_k X \ , \quad \mathscr{B}_k = X^{-1}B_k \ . \tag{22}$$

One can construct X by solving the first equation of (22). If $i = 0$, it follows from (15) that X diagonalises Γ^0 into Λ^0. This equation specifies X up to left multiplication by a diagonal matrix. The equation for $i = 1$, which relates Γ^1 into Λ^1, not only fixes the ambiguity, but also leads to an overdetermined system for the entries of X. Case-by-case analysis (up to $M = 6$ [16]) shows that the system admits a solution if and only if $s_{aa} = 1 + x_a^2 - 2\Delta\, x_a$, or, in other words, the R-matrix solves the Yang-Baxter equation.

5. Conclusions

In this report, we have summarised the results of [16], which presented closed formulae for the quantum gates of the ABC, proved the unitarity of such quantum gates, and worked out the equivalence between ABA and CBA through MPS. The results hint at several lines of research, some of which we comment on below.

The ABC produces states indepedently from the Bethe equations. The Bethe equations must be imposed by hand for the Bethe wave functions to be eigenstates of the Hamiltonian (2). One may reverse the situation and use the variational quantum eigensolver (VQE) to solve the Bethe equations.

Quantum gates simplify at the non-interacting point, where [15] showed they decompose into a layer of matchgates that is entirely determined by the sector with $r = 1$ for arbitrary $M \geq 1$. With the analytical expressions of [16] at hand, the question of whether a general decompositionn of the quantum gates of the ABC into one-qubit and two-qubit quantum gates is achievable arises.

Acknowledgments

This work as been supported by the Spanish MINECO grant PID2021-127726NB-I00. The author has been supported by the Universidad Complutense de Madrid, Ministerio de Universidades, and the European Union - NextGenerationE through contract CT18/22.

References

[1] Bethe H 1931 *Z. Phys.* **71** 205–226
[2] Korepin V E, Bogoliubov N M and Izergin A G 1993 *Quantum Inverse Scattering Method and Correlation Functions* Cambridge Monographs on Mathematical Physics (Cambridge University Press)
[3] Faddeev L D 1996 *Les Houches School of Physics: Astrophysical Sources of Gravitational Radiation* 149 (*Preprint* hep-th/9605187)
[4] Alcaraz F C and Lazo M J 2004 *J. Phys. A* **37** L1–L7 (*Preprint* cond-mat/0304170)
[5] Alcaraz F C and Lazo M J 2004 *J. Phys. A* **37** 4149–4182 (*Preprint* cond-mat/0312373)
[6] Alcaraz F C and Lazo M J 2006 *J. Phys. A* **39** 11335 (*Preprint* cond-mat/0608177)
[7] Katsura H and Maruyama I 2010 *J. Phys. A* **43** 175003 (*Preprint* 0911.4215)
[8] Murg V, Korepin V E and Verstraete F 2012 *Physical Review B* **86** ISSN 1550-235X (*Preprint* 1201.5627)
[9] Arute F, Arya K, Babbush R, Bacon D, Bardin J C, Barends R, Biswas R, Boixo S, Brandao F G S L and Buell D A t 2019 *Nature* **574** 505–510
[10] Hastings M B 2007 *J. Stat. Mech.* **0708** P08024 (*Preprint* 0705.2024)
[11] Verstraete F and Cirac J I 2006 *Physical Review B* **73** 094423–
[12] Van Dyke J S, Barron G S, Mayhall N J, Barnes E and Economou S E 2021 *PRX Quantum* **2** 040329 (*Preprint* 2103.13388)
[13] Van Dyke J S, Barnes E, Economou S E and Nepomechie R I 2022 *J. Phys. A* **55** 055301 (*Preprint* 2109.05607)
[14] Li W, Okyay M and Nepomechie R I 2022 *J. Phys. A* **55** 355305 (*Preprint* 2201.03021)
[15] Sopena A, Gordon M H, García-Martín D, Sierra G and López E 2022 *Quantum* **6** 796 (*Preprint* 2202.04673)
[16] Ruiz R, Sopena A, Gordon M H, Sierra G and López E 2023 The Bethe Ansatz as a Quantum Circuit (*Preprint* 2309.14430)